

Phenomena of Multiarc Roots and Parallel Arcs in a Large-Scale Magnetically Rotating Arc Plasma Generator

Jun Zha, Xiaoning Zhang, Zimu Xu, Cheng Wang, Beihe Du, and Weidong Xia

Abstract—Multiarc roots on the anode and parallel arcs occur in a magnetically rotating arc plasma generator. Appearance of these multiarc roots on the anode was once attributed to either arc shunting or parallel arcs. However, it has been observed that they all originate from dispersed arc plasmas (DAPs) in large-scale magnetically rotating arc plasma generators. Parallel dual arcs begin with the formation of contracted arc roots which then contract and grow in the DAP. There can be up to six multiarc roots on the anode. The coexistence time of parallel dual arcs is generally about 2–3 ms, and the maximum duration time is 9 ms. The characteristics of these multiarc roots and parallel arcs, such as their external parameters, configuration, luminosity, and arc voltage, are discussed throughout their generation, evolution, and extinguishment phases.

Index Terms—Magnetically rotating arc plasma, multiarc roots, parallel arcs.

I. INTRODUCTION

MULTIARC roots [1]–[7], which are spots of the arc column attached to the anode wall, occur in a magnetically rotating arc plasma generator. Most of the multiarc roots have been attributed to instantaneously existing “arc shunting” [1], [2]. Dorier *et al.* [2] investigated the arc fluctuation in Sulzer Metco F4-type dc plasma gun and observed the processes of creation and disappearance of multiattachments. Attachments (of up to three) have been observed to coexist during the 1- μ s exposure time of the camera under 500-A current and H₂/Ar gas flow rates of 4/40 SLPM. The mechanisms of the successive multicoexisting attachments, however, have not been successfully revealed until now. Multiarc roots of the shunting arc are dominated by the breakdown between the arc column and the anode wall in a magnetically rotating arc plasma generator, as typically shown in Fig. 1 [12]. “Arc shunting” may correspond to the “arc restrike mode” of the plasma torch introduced in [1], [8]–[11]. Arc reattachment on the anode is initiated by

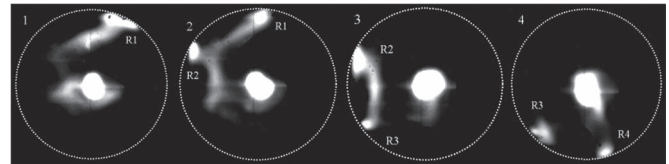


Fig. 1. Multiarc roots of arc shunting ($I = 150$ A, $B = 1.2$ mT, 100- μ s shutter, and 1000 fps).

a streamerlike breakdown, and the new arc root is formed upstream.

Recently, the use of the phenomenon of coexisting parallel arcs to explain the existence of multiarc roots has gained popularity. In addition, coexisting parallel arcs have the additional benefit of reducing the amount of electrode ablation [3]–[7]. Mino *et al.* [3] observed a mass of “splitting arcs” in a magnetically rotating arc plasma generator (400-A arc current, 450-A magnetic coil current, and 50-g/s gas flow rate) with the aid of a high-speed digital camera (exposure time: 20 μ s). According to their research, the parallel arcs coexist for about 0.1 ms. In fact, they are distinct from “multiarc roots” in images in the publication. Desaulniers and Meunier [4] observed by spectroscopic methods with an interelectrode gap of 5.15 mm and a magnetic field intensity of 0.1 T that the mean number of arc channels is 1.1–1.3. Essiptchouk *et al.* [5] produced a new formula for the arc rotational velocity. The formula has good agreement with experimental results with smaller interelectrode gaps but fails with larger interelectrode gaps. If one assumes that a single arc splits into two parallel arc columns and currents in each arc column decrease to half of the original, there is good agreement between the experimental points and the theoretical profile. By using a commercial CCD camera (15 fps and 100- μ s shutter), Li has obtained successive images on which two or three arc roots are observed [6], [7]. Li inferred that there are multiple coexisting parallel arcs in these images because the luminosity and the diameter of the arc columns are different from those in arc shunting [7].

Although the phenomena of multiarc roots and parallel arcs have been investigated in previous research, there has been a lack of adequate experimental evidence and detail in the studies of these valuable phenomena. In a large-scale magnetically rotating arc plasma generator with an arc chamber of 80-mm diameter, called the large-area dispersed arc plasma (DAP) source [12], completely dispersed arc plasma clouds and diffusive arc roots have been obtained under relatively high current and magnetic field intensity (400 A and 12 mT) [1],

Manuscript received August 30, 2012; revised November 29, 2012, January 17, 2013, and January 18, 2013; accepted January 18, 2013. Date of publication February 22, 2013; date of current version March 7, 2013. This work was supported by the National Natural Science Foundation of China under Grants 50876101, 11035005, and 10675122.

J. Zha, X. Zhang, Z. Xu, C. Wang, and W. Xia are with the Department of Thermal Science and Energy Engineering, University of Science and Technology of China, Hefei 230027, China (e-mail: zhajun@mail.ustc.edu.cn; zxn@mail.ustc.edu.cn; xzm@mail.ustc.edu.cn; awcheng@mail.ustc.edu.cn; xiawd@ustc.edu.cn).

B. Du is with the China Aerodynamics R&D Center, Mianyang 621000, China (e-mail: dubh@ustc.edu).

Color versions of one or more of the figures in this paper are available online at <http://ieeexplore.ieee.org>.

Digital Object Identifier 10.1109/TPS.2013.2243474

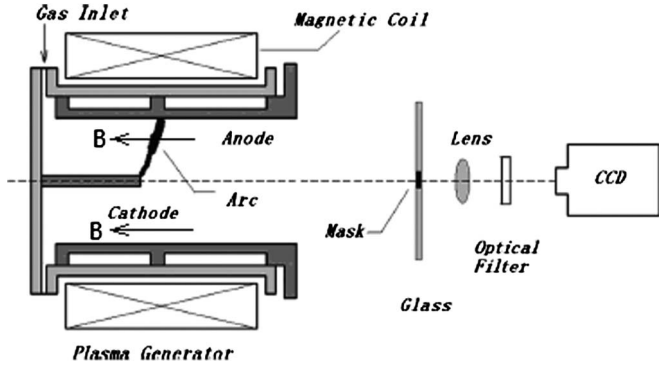


Fig. 2. Schematic representation of the experimental setup.

[12]–[16]. In this paper, we show that DAP and contracted arc columns coexist and intertransform under the condition of low current and magnetic field intensity (300 A and 6 mT) and so do diffusive anode attachments and contractive multiarc roots. A large number of successive images of multiarc roots and parallel arcs were captured by a high-speed CCD camera. Up to six multiarc roots are observed at any given moment, and the maximum duration time of the parallel arcs is about 9 ms. Characteristics of these multiarc roots and parallel arcs are discussed hereinafter, such as their external parameter, configuration, luminosity, and arc voltage, during their generation, evolution, and extinguishment phases.

II. EXPERIMENTAL APPARATUS

The experimental device employed in this work is shown in [8], as also shown in Fig. 2. The plasma generator is constructed with an anode chamber (80-mm diameter, 260-mm length, and graphite). One end of the chamber was covered with a flange, while the other was open to the atmosphere. A concentric cathode (18-mm diameter, 160-mm length, and graphite) has one end fixed to the center of the flange. An external solenoid coil produces axial magnetic fields in the chamber to rotate the arc. The arc current ranges from 100 to 400 A, and the magnetic field intensity is 2–20 mT. Argon gas axially flows from the end of the flange to the open end of the chamber, and the flow rate is $3 \text{ Nm}^3/\text{h}$. A high-speed CCD camera is positioned opposite to the open end of the generator, by which continuous end-on images of arcs and arc motion are captured. The recording frame rate ranged between 1000 and 5000 fps, and the exposure time ranged between 1 and $10 \mu\text{s}$. The arc voltages are synchronously measured with the arc images. The flange surface inside the generator has been painted black in order to reduce the reflection. To improve the definition and contrast of the arc columns, a specially designed mask intercepts the light emitted from the hot cathode. A voltage divider and a 100-kHz wideband DAQ card are utilized to acquire the arc voltage signals. Due to the difficulty in measuring the current signals in each of the parallel arcs, currents and their intertransfer between parallel channels were roughly estimated in terms of the variation of the arcs' thickness and luminosity.

Consecutive arc images and the waveforms of the arc voltage at different times in one experiment are shown in Figs. 3–6 with an axial magnetic field intensity of 6 mT, arc currents of 300 A,

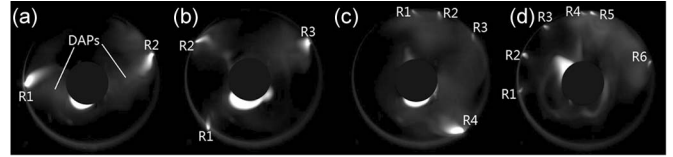


Fig. 3. Multiarc roots of different numbers ($I = 300 \text{ A}$, $B = 6 \text{ mT}$, and $G = 3 \text{ Nm}^3/\text{h}$).

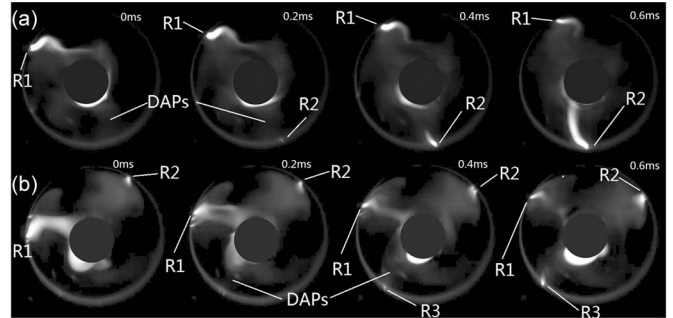


Fig. 4. Continuous images of the formation of multiarc roots ($I = 300 \text{ A}$, $B = 6 \text{ mT}$, and $G = 3 \text{ Nm}^3/\text{h}$).

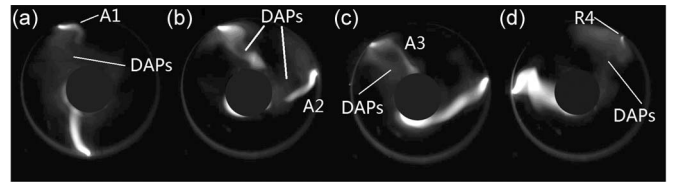


Fig. 5. Images of parallel arcs ($I = 300 \text{ A}$, $B = 6 \text{ mT}$, and $G = 3 \text{ Nm}^3/\text{h}$).

and an argon gas flow of $3 \text{ Nm}^3/\text{h}$. The CCD camera frame rate was 5000 fps, and the exposure time was $1 \mu\text{s}$. The sampling frequency of the DAQ was 25 kHz. In these images, the outer luminous annuli represent the opening of the plasma chamber, and the central black spots indicate the cathode luminescence obscured by the mask. The arcs rotate clockwise in Lorentz force direction.

III. RESULTS AND DISCUSSION

A. Multiarc Roots

Fig. 3 shows images of typical multiarc roots of different numbers. The brightness and contrast of the image have been adjusted so that DAPs [12]–[16] are more visible. The DAP clouds are shown not to be artifacts produced by the fast moving arc by comparing the $1\text{-}\mu\text{s}$ exposure time of the camera (5000 fps) with the arc rotating speed (about $\pi/6 \text{ rad/ms}$). In these images, the DAP clouds fill most of the cross-sectional area of the chamber and have distinct diffusive attachments on the anode. A few luminous arc columns exist close to the anode and the cathode but not through the interelectrode gap. The luminous spots attached to the anode are immersed in DAPs, which are thought of as multiarc roots.

Fig. 3(a) and (b) shows two and three contractive arc roots on the anode, respectively. Compared with the DAPs in Fig. 3(c) and (d), the latter occupy larger area and are less constricted on the anode surface. As a result, more arc roots may coexist.

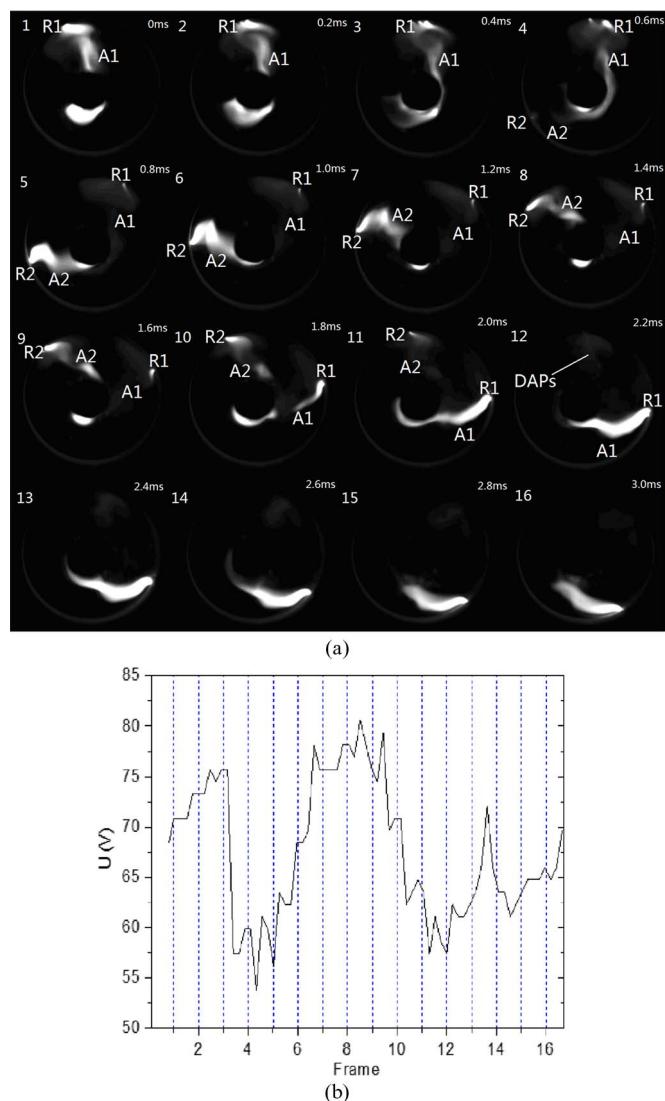


Fig. 6. (a) Images of parallel arcs evolving ($I = 300$ A, $B = 6$ mT, and $G = 3$ Nm^3/h). (b) Synchronous arc voltage corresponding to (a) (sampling frequency = 25 kHz).

Six arc roots are shown in Fig. 3(d), which is the most that we have captured. As the number of arc roots increases, their size, luminosity, and coexistence times decrease. Most frequently, dual arc roots occur and coexist for the maximum duration (often 2–3 ms, up to 9 ms). Triple arc roots coexist for less than 1 ms, and the coexistence time of the six arc roots is less than 0.2 ms, which is limited by the refresh frame rate of the CCD camera.

Fig. 4 shows successive images of two groups [(a) and (b)] of the multiarc root generation phase. All the images in Fig. 4 demonstrate that the multiarc roots on the anode originated from the DAPs. In Fig. 4(a), for example, two contracted arc roots on the anode from frame 2 to frame 4 are immersed in the DAPs with obviously diffusive attachments to the anode. The arc root R1 exists from frame 1 to frame 4 while the arc root R2 emerges in frame 2 and lasts to frame 4. Before R2 formed, a large number of DAPs appeared around R2 (frames 1 and 2). Fig. 4(b) shows a similar situation of a third arc root occurring. They are also immersed in DAPs with diffusive attachment to

the anode. It should be noticed that R1 splits into three small roots in frame 2 while R2 splits into two in frame 3.

Generally, most multiarc roots are formed by partial shrinking of the DAPs with diffusive arc attachment to the anode. They are likely caused by instability of the arc plasma near the anode. It has been observed that the breakdown between the DAPs and the anode may also lead to the formation of multiarc roots (Section III-C).

B. Parallel Arcs

Parallel arcs were generally thought to consist of multiple independent arc columns through interelectrodes [8], [11]. However, it has been found that there are few full columns of parallel arcs through interelectrodes in the large-scale magnetically rotating arc plasma generator while the ever-present DAPs are part of them. Furthermore, most contracted parallel arc columns are immersed in the DAPs. They originate from either the shrinking of the DAPs or dispersal into the DAPs. Fig. 5(a)–(d) shows several typical parallel dual arcs. Parts of the columns of parallel arcs were found to be not luminous. Interelectrode arc columns A1 and A2 in Fig. 5(a) and (b), respectively, are partly dispersed. In Fig. 5(c), we find arc column A3 immersed in the DAPs. Fig. 5(d) shows that the most extreme status of the parallel arcs consists of one arc column and a piece of DAP with a small contracted anode arc root R4.

Thus, in our experiments, the alleged “parallel arcs” consist of multicontracted luminous anode arc roots and one or more relatively luminous arc columns while parts of which may be dispersed. The “parallel dual arcs” with full contractive arc columns are typical “parallel arcs.” Nevertheless, we find no more than two full arc columns coexisting. Furthermore, the two columns of the parallel dual arcs may be dispersed during the coexistence time of multiarc roots. As a result, the duration of parallel dual arcs is often shorter than that of the multiarc roots. This phenomenon is discussed in more detail later in Section III-C.

C. Evolution of the Parallel Dual Arcs

The phenomenon of “parallel dual arcs,” which consists of not only the contracted and luminous arc roots but also arc columns, is a typical representation of multiarc roots. Moreover, this phenomenon begins with the formation of two contracted luminous anode arc roots and ends with extinguishment of one of the contractive arc roots. In this section, the phases of the generation, evolution, and extinguishment of the parallel dual arcs, and their relations to multiarc roots, are discussed.

Successive images of the evolution phase of the parallel dual arcs and the corresponding waveforms of arc voltage are shown in Fig. 6(a) and (b), respectively.

In frames 1–3, there are one arc root R1 and a column A1. A1 is dispersed while the arc voltage rises gradually from 68 to 75 V. That implies that the conductivity of the contracted arc column is greater than that of the DAP. In frame 4, the new arc root R2 emerges in another piece of the DAP, and it is seen that R2 might be generated by the breakdown between the DAP

and the anode. However, R1 and A1 of the arc continue to exist while the new arc root R2 forms, which is also the initiation of “parallel dual arcs.”

Initiation of a new contracted arc root is always accompanied by arc voltage drop. The arc voltage drops from 75 to 59 V in 0.04 ms during the formation period of R2 between frame 3 and frame 4. This implies that the conductivity of the arc root steeply rises due to its contraction.

Following R2's emergence in frame 4, the contracted luminous arc column A2 is rapidly formed from the DAP in frame 5, while A1 keeps on dispersing and R1 keeps on contracting until frame 8. It may be inferred that currents in A2 increase. From frame 5 to frame 8, the contracted arc column A2 disperses gradually, accompanied with the rising arc voltage. The contracted arc column A2 rotates and arc root R2 moves about $\pi/6$ rad around the central angle in 0.6 ms, while R1 rotates more slowly than R2.

From frame 9 to frame 12, A2 remains dispersed, while A1 transforms into a contracted luminous arc column again which becomes thicker and brighter; the corresponding arc voltage drops gradually from 75 to 58 V in 0.6 ms. R1 rotates faster than R2. It is inferred that currents in A2 transfer back into A1. In frame 12, R2 extinguishes, while the DAP exists with diffusive attachment on the anode until frame 16. The extinguishment of R2 indicates the end of the “parallel dual arcs” in frame 12.

Generally, the formation of the new parallel dual arcs starts with new contracted arc roots, which originate in a DAP with a diffusive attachment on the anode, and then, the luminous arc column extends from the root in the DAP. In turn, usually, the parallel dual arcs disappear with the arc column dispersing first and the contracted luminous arc root then diffusing, in our experiments.

In our experiments, the coexistence time of parallel dual arcs is often about 2–3 ms, and the maximum duration time is 9 ms. During the coexistence time, the contracted and dispersed arc columns may undergo more than two cycles.

D. Effects of the External Parameter on Multiarc Roots and Parallel Arcs

From our study, the magnetic field, gas flow, and electrodes are all able to influence the parallel arc occurrence and duration. We have investigated the initiation and stability of parallel arcs under the following experimental conditions: arc currents I from 100 to 400 A and axial magnetic field intensity B of 2–20 mT. The argon flow rate G is 3 or 6 Nm³/h.

With the arc currents ranging from 200 to 400 A, it was found that the multiarc roots and parallel arcs appear more frequently under the condition of $0.24 < I \cdot B < 4.8 \text{ A} \cdot \text{T}$ with a gas flow rate of 3 Nm³/h. When $I \cdot B > 4.8 \text{ A} \cdot \text{T}$, the DAP cloud which fills the entire chamber cross section can be sustained at high temperature and input power [12]. Additionally, the arc column shows a typical swirl shape with the contracting anode root when $I \cdot B < 0.24 \text{ A} \cdot \text{T}$ (200 A and 1.2 mT) [12]. Parallel arcs have not been observed with gas flow rates of 6 Nm³/h. The increase of the gas flow rate disturbs the initiation and stabilization of parallel arcs.

IV. CONCLUSION

In the large-scale magnetically rotating arc plasma generator, many images of continuous multiarc roots and parallel arcs have been captured. The characteristics of multiarc roots and parallel arcs have been investigated in this paper.

Generally, multiarc roots originate from the contraction of the DAPs with diffusive attachments to the anode wall or from the breakdown between the DAPs and the anode. Parallel dual arcs start with new contracted arc roots, and from those roots, contracted arc columns grow in the DAP. While the contracted arc columns are dispersed, the contracted arc root diffuses or extinguishes, reversing the process.

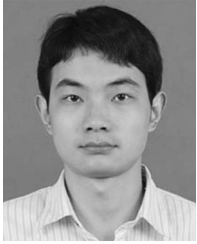
While the plasma arc (including its root or its column) was shrinking, the conductivity of plasma increased markedly which caused the arc voltage to drop. In turn, the dispersing contracted arc columns or arc roots were accompanied by an arc voltage rise.

According to our experiments, the coexistence time of parallel dual arcs is often about 2–3 ms, and the maximum duration time is 9 ms. The multiarc roots and parallel dual arcs would appear more preferentially under the experimental conditions of arc currents $200 < I < 400 \text{ A}$ and $0.24 < I \cdot B < 4.8 \text{ A} \cdot \text{T}$ at an argon flow rate $G = 3 \text{ Nm}^3/\text{h}$.

REFERENCES

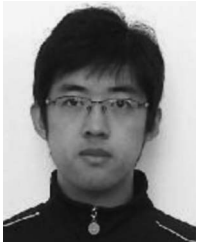
- [1] A. E. Guile, *Proc. Inst. Elect. Eng.*, vol. 118, no. 9, pp. 1131–1154, Sep. 1971.
- [2] J.-L. Dorier, M. Gindrat, C. Hollenstein, A. Salito, M. Loch, and G. Barbezat, “Time-resolved imaging of anodic arc root behavior during fluctuations of a DC plasma spraying torch,” *IEEE Trans. Plasma Sci.*, vol. 29, no. 3, pp. 494–501, Jun. 2001.
- [3] H. Minoo, A. Arsaoui, and A. Bouvier, “An analysis of the cathode region of a vortex-stabilized arc plasma generator,” *J. Phys. D, Appl. Phys.*, vol. 28, no. 8, pp. 1630–1648, Aug. 1995.
- [4] N. S. Desaulniers and J. L. Meunier, “A study of magnetically rotating arc stability using fluctuations in voltage, velocity and emission line intensity,” *J. Phys. D, Appl. Phys.*, vol. 28, no. 12, pp. 2505–2513, Dec. 1995.
- [5] A. M. Essiptchouk, L. I. Sharakhovsky, and A. Marotta, “A new formula for the rotational velocity of magnetically driven arcs,” *J. Phys. D, Appl. Phys.*, vol. 33, no. 20, pp. 2591–2597, Oct. 2000.
- [6] H. Li, “The model of arc plasma in cathode region and research of the auxiliary heated arc plasma generator,” Ph.D. dissertation, Univ. Sci. Technol. China, Hefei, China, 2000.
- [7] H. Li, Q. Ma, L. C. Li, and W. D. Xia, “Imaging of behavior of multiarc roots of cathode in a dc arc discharge,” *IEEE Trans. Plasma Sci.*, vol. 33, no. 2, pp. 404–405, Apr. 2005.
- [8] J. P. Trelles, C. Chazelas, A. Vardelle, and J. V. R. Heberlein, “Arc plasma torch modeling,” *J. Therm. Spray Technol.*, vol. 18, no. 5/6, pp. 728–752, 2009.
- [9] S. A. Wutzke, E. Pfender, and E. R. G. Eckert, “Symptomatic behavior of an electric arc with a superimposed flow,” *AIAA J.*, vol. 6, no. 8, pp. 1474–1482, Aug. 1968.
- [10] J. F. Coudert, M. P. Planche, and P. Fauchais, “Characterization of d.c. plasma torch voltage fluctuations,” *Plasma Chem. Plasma Process.*, vol. 16, no. 1, pp. S211–S227, Mar. 1995.
- [11] Z. Duan and J. V. R. Heberlein, “Arc instabilities in a plasma spray torch,” *J. Therm. Spray Technol.*, vol. 11, no. 1, pp. 44–51, Mar. 2002.
- [12] W. D. Xia, L. C. Li, B. H. Du, Y. H. Zhao, Q. Ma, L. Cheng, and Q. Chen, “Dynamics of large-scale magnetically rotating arc plasmas,” *Appl. Phys. Lett.*, vol. 88, no. 21, pp. 211501-1–211501-3, May 2006.
- [13] L. C. Li, W. D. Xia, H. L. Zhou, and B. Bai, “Experimental observation and numerical analysis of arc plasmas diffused by magnetism,” *Eur. Phys. J. D*, vol. 47, no. 1, pp. 75–81, Apr. 2008.
- [14] H.-L. Zhou, L.-C. Li, L. Cheng, Z. P. Zhou, B. Bai, and W. D. Xia, “ICCD imaging of coexisting arc roots and arc column in a large-area dispersed arc-plasma source,” *IEEE Trans. Plasma Sci.*, vol. 36, no. 4, pp. 1084–1085, Aug. 2008.

- [15] L.-C. Li, Q. Chen, H.-L. Zhou, and W. D. Xia, "Images of a large-scale magnetically rotating arc," *IEEE Trans. Plasma Sci.*, vol. 36, no. 4, pp. 1080–1081, Aug. 2008.
- [16] H.-L. Zhou, Z.-P. Zhou, L.-C. Li, L. Cheng, B. Bai, and W. D. Xia, "Investigation of a novel large area dispersed arc plasma source with time-resolved ICCD imaging," *IEEE Trans. Plasma Sci.*, vol. 36, no. 4, pp. 1082–1083, Aug. 2008.



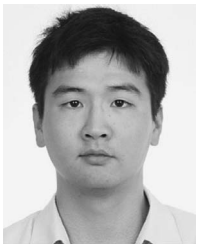
Jun Zha was born in Anqing, China, in 1986. He received the B.E. degree from the University of Science and Technology of China, Hefei, China, in 2008, where he is currently working toward the Ph.D. degree.

His research interest is focused on the diagnostics and the application of the arc plasma.



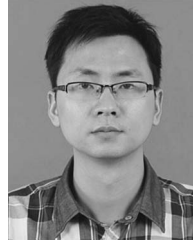
Xiaoning Zhang was born in Weihai, China, in 1986. He received the B.E. degree from the University of Science and Technology of China, Hefei, China, in 2009, where he is currently working toward the Ph.D. degree.

His research interest includes the study of nonequilibrium thermal plasmas.



Zimu Xu was born in Hefei, China, in 1988. He received the B.S. degree from the University of Science and Technology of China, Hefei, in 2010, where he is currently working toward the Ph.D. degree.

His research interest includes the application of nonthermal plasma in medicine.



Cheng Wang was born in Chongqing, China, in 1987. He received the B.E. degree from the University of Science and Technology of China, Hefei, China, in 2010, where he is currently working toward the Ph.D. degree.

His research interest includes the application of the arc plasma.



Beihe Du was born in Pingliang, China, in 1970. He received the M.E. degree from the University of Science and Technology of China, Hefei, China, in 2005.

He is currently a Senior Researcher with China Aerodynamics R&D Center, Mianyang, China. His main interests are the interaction mechanism between arc plasma and thermal protection material.



Weidong Xia was born in Hefei, China, in 1959. He received the Ph.D. degree from the Institute of Plasma Physics, Chinese Academy of Sciences, Hefei, in 1990.

He is currently the Head of the Applied Plasma Laboratory, University of Science and Technology of China, Hefei. His main interests are the application of the arc plasma and nonthermal plasma.